Chemical Engineering Journal 101 (2004) 171–178

Chemical Engineering Journal

www.elsevier.com/locate/cej

Feasibility study on concentration of slurry and classification of contained particles by microchannel

Shinichi Ookawara [a,*], Ryochi Higashi [a], David Street [b], Kohei Ogawa [a]

[a] *Department of Chemical Engineering, Graduate School of Science and Technology, Tokyo Institute of Technology, Tokyo 152-8552, Japan*
[b] *Fluent Asia Pacific, Tokyo 160-0023, Japan*

Abstract

The feasibility of a newly developed micro-separator/classifier is examined numerically and experimentally. The main section of the device is a curved channel with a rectangular cross-section, which has a bifurcation at one end. The width, depth and curvature radius of the channel are 200 μm, 170 μm and 20 mm, respectively. This geometry creates secondary flow patterns called Dean vortices. The concentration and classification are thought to be caused by the balance of high centrifugal acceleration that traps particles near outer wall and the intensity of Dean vortices that enhance mixing and re-dispersion of particles in the secondary flow field. Although the residence time is extremely short because of the channel size, it is confirmed by numerical simulations that secondary flow patters are established immediately after entering the curved section and that the channel is long enough that several circulations are expected for re-dispersion. Suspensions, whose weight concentration is 0.06 wt.%, are prepared as test fluids using ion-exchanged water and acrylic polydisperse particles whose average diameters are 7, 10 and 20 μm, respectively. It is experimentally confirmed that the structure results in concentration and classification for the all particles in the *Re* range of 150–600 (the *De* range of 10–40). It is also verified that the efficiencies increase with the particle size.

Keywords: Microchannel; Separation; Classification; Particle; Suspension

1. Introduction

Research and development for the production of fine particles using a microreactor is receiving much attention by many researchers [1–3], especially to achieve monodispersity and well-controlled morphology by taking advantages of high selectivity, mass and heat transfer rates. In the case that desirable properties are not sufficiently achieved in a microreactor, downstream unit operations such as concentration, separation, classification are also needed. Since the flow rate of the slurry is generally very small the application of available apparatus such as classical hydrocyclones are unsuitable because of their huge volume compared with that of the microreactor. Even the smallest mini-hydrocyclone [4] currently available whose diameter is 1 cm, has an operating flow rate of approximately 150 l/h and would not be suitable as a microseparation device.

Therefore, demand exists for a microdevice for the concentration of slurry and the classification of particles suitable for a new breed of microreactor. Except for work of Shelby et al. [5] there is very little literature available describing such microdevices. It is desirable to perform such unit operations in a microdevice that can be directly connected to the upstream microreactor to create a so-called chemical "microplant". Based on this motivation, the feasibility of a novel curved microchannel is examined both numerically and experimentally in this paper.

2. Concept of micro-separator/classifier

Fig. 1 depicts the concept of the proposed micro-separator/classifier. The main section is a curved microchannel with a rectangular cross-section whose width, depth and the curvature radius in this study are 200 μm, 170 μm and 20 mm, respectively. At the inlet the particles are dispersed homogeneously. While passing through the channel, particles are exposed to a high centrifugal force because of the high tangential velocity and a small radius of curvature. For instance, a flow rate of 6.12 ml/min results in a mean velocity and centrifugal acceleration of 3 m/s and 450 m/s^2 over the cross-section, respectively. The high centrifugal acceleration is expected to work in favor of concentrating particles

* Corresponding author. Tel.: +81-3-5734-3035; fax: +81-3-5734-2882.
E-mail address: sokawara@chemeng.titech.ac.jp (S. Ookawara).

1385-8947/$ – see front matter © 2003 Elsevier B.V. All rights reserved.
doi:10.1016/j.cej.2003.11.008

Nomenclature

a_{ave}	average centrifugal acceleration over the cross-section of microchannel
a_{max}	maximum centrifugal acceleration over the cross-section of microchannel
D	particle diameter
D_{eq}	equivalent diameter of microchannel
D_{in}	average diameter of particles contained in slurry obtained from inner exit ports
D_{out}	average diameter of particles contained in slurry obtained from outer exit ports
De	Dean number
I_{in}	absorbance at 900 nm of slurry obtained from inner exit ports
I_{out}	absorbance at 900 nm of slurry obtained from outer exit ports
R	curvature of curved section of microchannel
Re	Reynolds number
T_C	circulation time of Dean vortex
T_R	residence time of fluid
U	mean tangential velocity over the cross-section of microchannel
U_{max}	maximum tangential velocity over the cross-section of microchannel
$V_{ave,Dean}$	average secondary flow velocity over the cross-section of microchannel
$V_{max,Dean}$	maximum secondary flow velocity over the cross-section of microchannel
V^*	non-dimensional average secondary flow velocity ($\equiv V_{ave,\,Dean}/U$)
$V^*_{critical}$	non-dimensional critical secondary flow velocity

Greek letters

μ	viscosity of suspending medium
ρ	density of suspending medium

near the outer wall of the channel. On the other hand, there exists another factor that also influences the distribution of particles. In a curved tube, secondary flow patterns called Dean vortices that are normal to the angular velocity appear over the cross-section as shown in Fig. 1. These Dean vortices enhance the re-dispersion of the particles in the slurry.

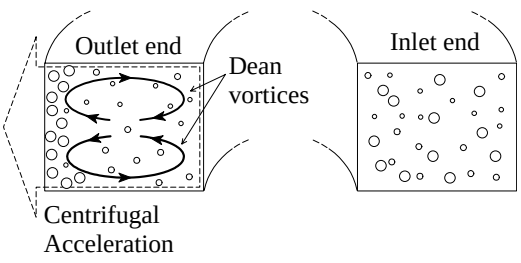

Fig. 1. The schematic diagram of separation/classification mechanism.

The balance of the centrifugal acceleration and the intensity of the Dean vortices will both influence the concentration distribution of slurry particles. If the centrifugal acceleration is high while the Dean vortices are extremely weak, only concentration effects will be apparent. Since the opposite factor that influence the particle behavior does not exist in this case, the micro-separator/classifier is similar to a centrifuge that results in phase separation based on the density differences, such as the microdevice developed by Shelby et al. [5], although their device seems to be suitable for the batch operation due to its physical structure. On the other hand, since the relative velocity between larger particles and the suspending medium is always larger than that between smaller particles and the medium, the larger particles will tend to be concentrated near outer wall while the smaller particles will tend to move along with the Dean vortices. Furthermore, the concentrated larger particles could exclude smaller particles from near the outer wall region by their physical volume. Therefore, smaller particles could exist near the inner wall rather than the outer wall or the concentration of smaller particles near the outer wall could be lower than for homogeneous state. If the channel has a bifurcation at the outlet end, then the larger particles flowing near the outer wall will be obtained mostly from the outer branch of the bifurcation, while the dispersed smaller particles will be obtained from both branches or possibly mostly from the inner branch. The principle is similar to that of cyclones in which larger particles are contained in the underflow by appropriate centrifugal acceleration while smaller particles are equally contained in both over- and underflow because of the small slip velocity with the suspending medium. It can be said that the nature of the micro-separator/classifier varies from that of centrifuges to cyclones according to the intensity of the Dean vortices. For micro-separator/classifier, however, the increase of operating flow rates possibly results in an excessive intensity of Dean vortices that re-disperse even larger particle. Therefore, there should be an optimum balance that causes a classification effect in the micro-separator/classifier. The balance will be changed by many factors such as the flow rate, the channel size and the channel aspect ratio. It is possible that the efficiency of concentration and classification can be controlled.

In the present work, the assumed mechanism described above will be examined numerically and experimentally as a first step before determining the optimum operating conditions. The establishment and the circulation frequency of the Dean vortices are especially important since this is crucial for the classification. For subsequent studies the magnitude of the centrifugal acceleration and the strength of the Dean's vortices are described using simple correlations. Since it is difficult to measure the flow patterns in tiny channels the flow patterns are modeled numerically using the commercial CFD code FLUENT 6.1. Finally, experimental evidence

will be shown for both the concentration effects and classification.

3. Numerical simulations

3.1. Numerical method

There are many factors that influence the performance of micro-classifier/separator such as the size, aspect ratio, shape and curvature of the channel; flow rate; size distribution, density and feed concentration of particles; viscosity, density and non-Newtonian properties of suspending medium, etc. First of all, a comprehensive understanding of the flow field and the particle behavior is crucial among for a reasonable separator design. In our experiments, the particle concentration is very low (0.06 wt.%) and the relative viscosity of the suspension is predicted to be about 1.001 based on Einstein's equation [6,7]. Therefore, it is supposed that presence of the particles does not significantly influence fluid properties and thus the flow field. As such the flow simulation performed without particles still brings fundamental information which can be used in the present study. The influence of the aspect ratio (= width/depth) on the performance for larger microchannels will be reported elsewhere [8]. The coupled particle and fluid flow modeling will be performed in future work.

The commercial CFD code FLUENT 6.1, which is based on the finite volume method, is employed for the simulation of steady-state flow without particles in the micro-classifier/separator. The governing equations are the Navier–Stokes equations and the equation of mass conservation for incompressible fluids. For the pressure–velocity coupling and discretization schemes for convection terms, the SIMPLE method with a second-order upwind scheme is adopted in this study, respectively. Fig. 2 shows the geometry and boundary conditions for the simulation. The geometry is identical to the microchannel used in experiments except for that the outer branch and throughholes are not modeled. The width of outer branch increases to twice that of the other sections slightly downstream. Although the change of width is originally made so that the concentrated slurry could flow without high pressure loss and clogging, the structure causes a difference of flow rates within the inner and the outer branches for a dilute suspension. The volumetric flow rate ratio between the inner and the outer exit branches of the separator is 1–2.125 and was chosen to match the experimental conditions. In the model this is specified as an outlet boundary condition. In the present study, the flow properties are analyzed at position half way around the curved section, viz. $\theta = 90^\circ$. Therefore, the difference is not so significant for the following discussion. At the inlet one end of the curved semicircle channel, a short but straight channel whose width, depth and length are 200 μm, 170 μm and 5 mm, is added. One end of the straight section forms the inlet which is fed with slurry using a throughhole. Since the diameter of the throughhole (5.5 mm) is much larger than the size of microchannel a uniform velocity profile at the inlet is assumed. Therefore, the uniform velocity U is specified at the inlet as boundary condition. In this study, the Reynolds number Re is defined as follows:

$$Re = \frac{\rho U D_{eq}}{\mu} \tag{1}$$

where D_{eq}, ρ and μ are the equivalent diameter, density and viscosity of water, respectively. Values of 1000 kg/m^3 and 0.001 Pa s are specified for the density and viscosity, respectively. Equivalent diameter D_{eq} is calculated as

$$D_{eq} = \frac{4(\text{width} \times \text{depth})}{2(\text{width} + \text{depth})} = 184\,\mu\text{m} \tag{2}$$

Examined Re numbers are 150, 300, 450 and 600. These Re numbers give De numbers of 10, 20, 30 and 40 defined as

$$De = Re\sqrt{\frac{D_{eq}}{2R}} \tag{3}$$

where R is the radius of curvature. This non-dimensional group is related to the instability of flow in a curved channel [9,10] and used for the correlation in this study. The no-slip condition is specified at other boundaries. The mesh densities are 10 μm per mesh over the cross-sectional plane and about 50 μm per mesh in the streamwise direction except for the bifurcation section. The numerical grid contained approximately 540 000 cells.

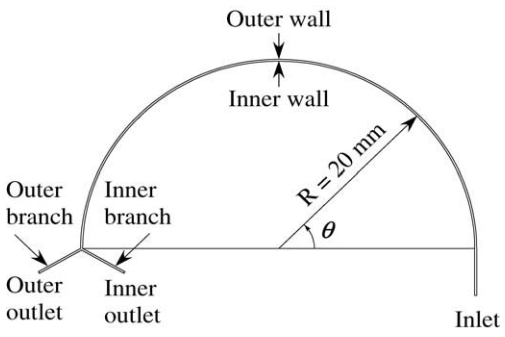

Fig. 2. The geometry and boundary definition for numerical simulation.

3.2. Results and discussion

Fig. 3 shows the development of maximum secondary flow velocity $V_{max,Dean}$ over the cross-section at an angular position θ. The $V_{max,Dean}$ rapidly increases with angle and reaches maximum value at $\theta = 6^\circ$ except for the case of $De = 10$. Even at $\theta = 4^\circ$, the $V_{max,Dean}$ exceeds the converged value for all cases. Although slight fluctuation can be seen for $De = 30$ and 40, it immediately converges to a constant value after passing the peak within 30° for all cases examined. Therefore, it is supposed that the secondary flow patterns are immediately established after entering the curved section and the re-dispersion effect starts to work very near the inlet region.

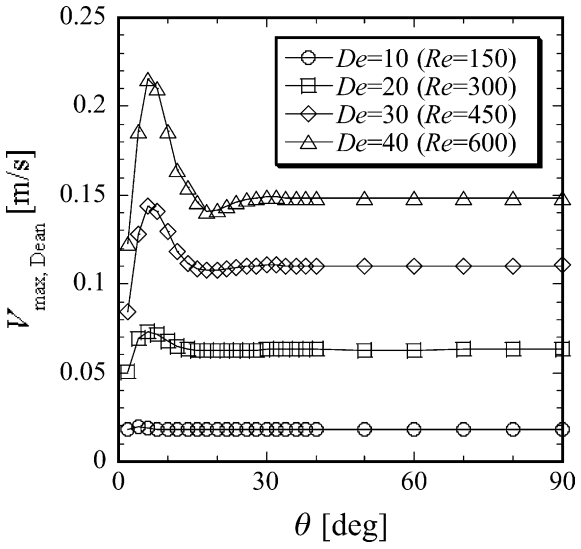

Fig. 3. The maximum secondary flow (Dean vortices) velocity at an angular position θ.

On the other hand, Fig. 4 shows the development of maximum tangential velocity U_{max} over the cross-section at an angular position θ. It can be seen that the U_{max} does not fluctuate so much compared with $V_{max,Dean}$ near the inlet region although the trend is similar. These results imply that secondary flow mainly works to shift the maximum velocity position outwards in the direction of centrifugal acceleration and not to increase the tangential velocity.

Fig. 5(a) and (b) shows the centrifugal acceleration profile of $De = 10$ and 40 in a vertical plane half way around the curved section, viz. $\theta = 90^\circ$. The left edge of the figure corresponds to the outer wall of the channel. It can be seen that the higher acceleration region shift outwards and the shape become longer rather than wider. This region corresponds to the high velocity region since the centrifugal acceleration at a point is calculated as squared tangential velocity

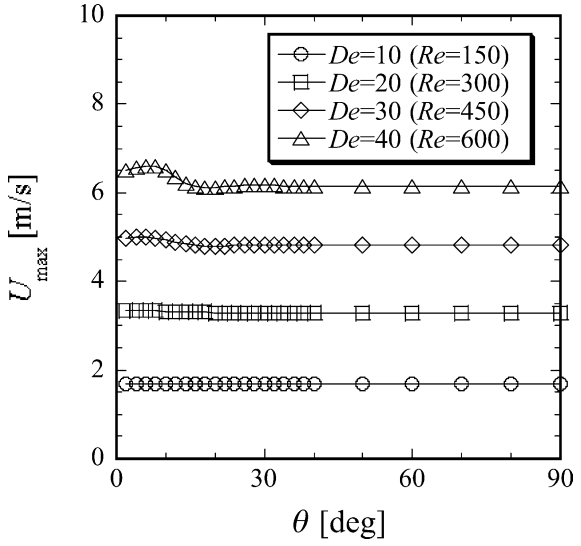

Fig. 4. The maximum tangential velocity at an angular position θ.

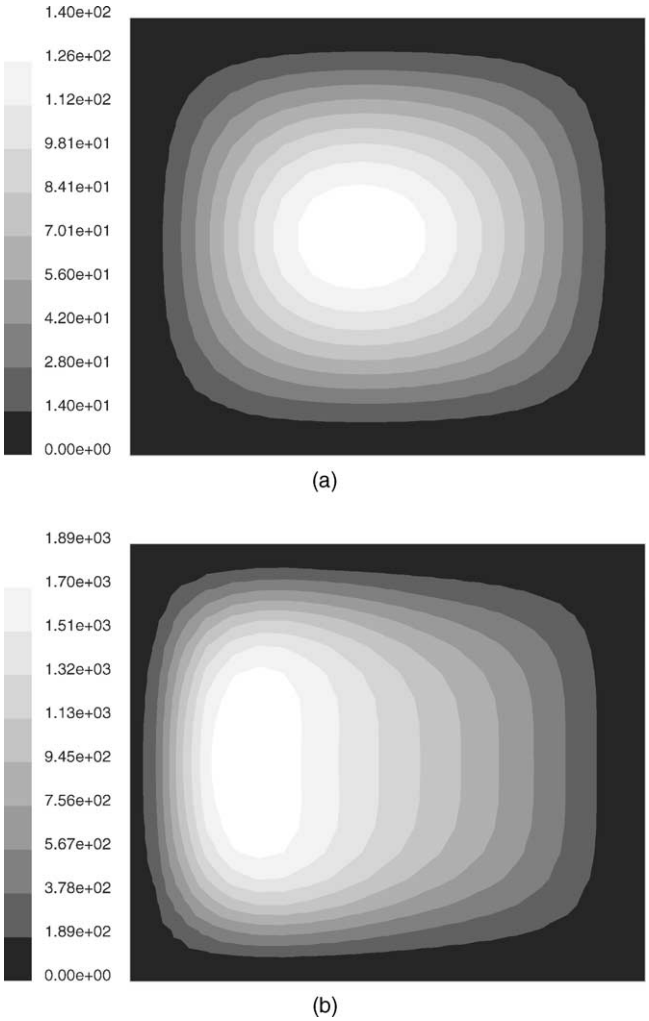

Fig. 5. The centrifugal acceleration profile of (a) $De = 10$ and (b) $De = 40$ in the plane at half way around the curved section, viz. $\theta = 90^\circ$.

divided by its radial position from the center of curvature at the point. As shown in Fig. 6, the average and the maximum centrifugal acceleration a_{ave} and a_{max} are expressed by the following correlations:

$$a_{ave} = 1.3\frac{U^2}{R} \quad (4)$$

$$a_{max} = 3.6\frac{U^2}{R} \quad (5)$$

Each coefficient is slightly larger than that for a larger microchannel with a high aspect ratio [8]. Therefore, it seems that the size and aspect ratio do not significantly change the magnitude of the centrifugal acceleration.

Fig. 7(a) and (b) shows the secondary flow vectors of $De = 10$ and 40 in the vertical plane half way around the curved section, viz. $\theta = 90^\circ$. It can be seen that Dean vortices appear in the cross-sectional plane for minimum and maximum flow rate conditions. The intensity apparently increases and the vortices shift outwards with increasing De and this corresponds with the change of centrifugal

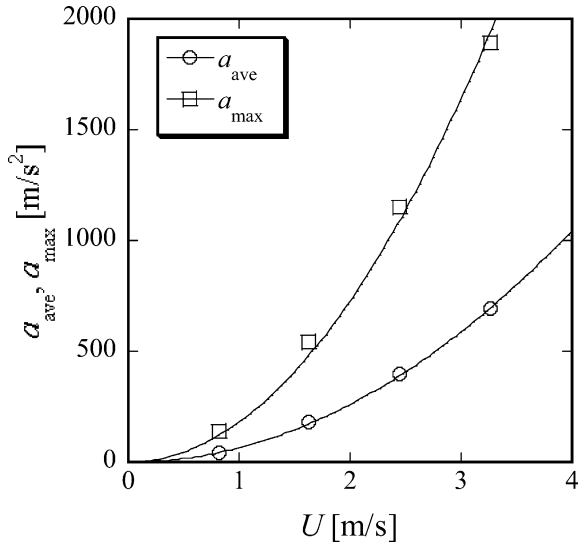

Fig. 6. The dependency of average and maximum centrifugal acceleration a_{ave} and a_{max} on mean velocity U at half way around the curved section, viz. $\theta = 90^\circ$.

acceleration profile. As shown in Fig. 8, the average and maximum secondary flow vector velocity $V_{ave,Dean}$ and $V_{max,Dean}$ are expressed by the following correlations:

$$V_{ave,Dean} = 1.8 \times 10^{-4} De^{1.63} \quad (6)$$

$$V_{max,Dean} = 3.9 \times 10^{-4} De^{1.63} \quad (7)$$

Although the exponents of Eqs. (6) and (7) are same as those of correlations obtained for a larger microchannel with high aspect ratio [8], the coefficients are significantly larger. Therefore, it is supposed that low aspect ratio enhances the secondary flow.

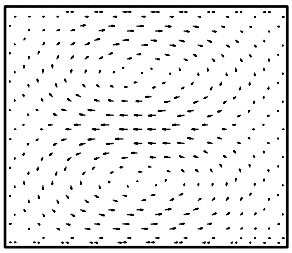

(a) De =10

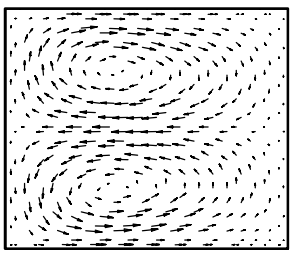

(b) De = 40

Fig. 7. The secondary flow vectors of (a) $De = 10$ and (b) $De = 40$ in the plane at half way around the curved section, viz. $\theta = 90^\circ$.

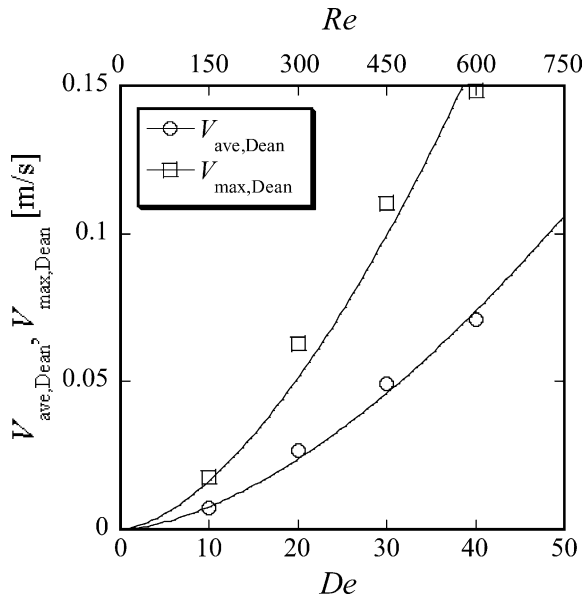

Fig. 8. The dependency of average and maximum secondary flow vector velocity $V_{ave,Dean}$ and $V_{max,Dean}$ on De number at half way around the curved section, viz. $\theta = 90^\circ$.

Fig. 9 shows the circulation model for the evaluation of the Dean vortices circulation frequency. It is assumed that vortices circulate at a velocity of $V_{ave,Dean}$ along with the circulation paths indicated by bold lines whose length is $3D_{eq}/2$. Accordingly, the time needed for a circulation T_C is calculated as

$$T_C = \frac{3D_{eq}}{2V_{ave,Dean}} \quad (8)$$

while the residence time in the curved section T_R is expressed as

$$T_R = \frac{\pi R}{U} \quad (9)$$

Therefore, more than one circulation is achieved when the following condition is satisfied:

$$\frac{T_R}{T_C} > 1, \quad \text{i.e. } \frac{V_{ave,Dean}}{U} \equiv V^* > \frac{3D_{eq}}{2\pi R} \equiv V^*_{critical} \quad (10)$$

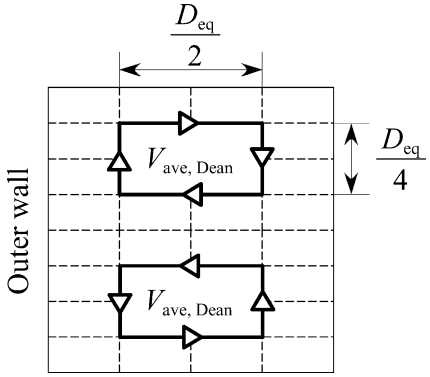

Fig. 9. The circulation model for the evaluation of circulation frequency of Dean vortices.

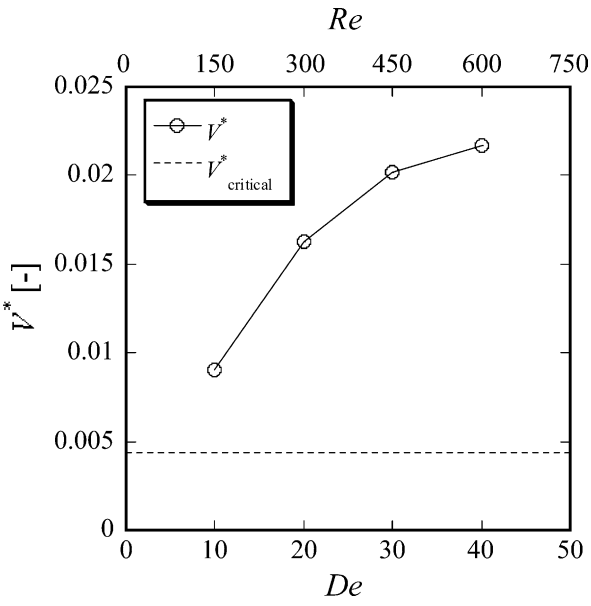

Fig. 10. The dependency of non-dimensional average and critical secondary flow velocity on *De*.

where V^* and V^*_{critical} are non-dimensional average and critical secondary flow velocity, respectively. The relation between V^* and *De* is shown as well as V^*_{critical} indicated by dotted line in Fig. 10. It can be seen that V^* increases with *De* and several circulations can be expected within the residence time for all the cases examined. It should be noted that the re-dispersion effect of the Dean vortices can be based on the above model in spite of a short residence time.

4. Experimental

4.1. Apparatus and experiments

Fig. 11 shows a schematic diagram of the experimental setup for the evaluation of micro-separator/classifier. It consists of a semicircle channel whose radius of curvature is 20 mm. The channel bifurcates at the end of the curved section. The outer branch becomes twice as wide as other

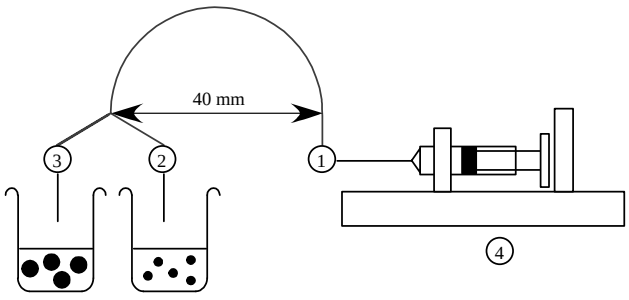

Fig. 11. The schematic diagram of experimental setup for the evaluation of micro-separator/classifier: (①) inlet throughhole; (②) inner exit throughhole; (③) outer exit throughhole; (④) microfeeder.

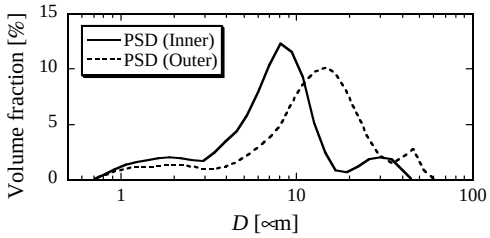

Fig. 12. Volume-based particle size distributions (PSD) of samples collected from inner and outer exits at $De = 40$ ($Re = 600$) for the 10 μm particles.

section at some distance downstream from bifurcation. The curved microchannel with bifurcation and straight entry section is designed by using CAD software (Rhinoceros, Robert McNeel & Associates) in this study. An engraving machine (EGX-300, Roland) equipped with a square end mill slots the microchannel on an acrylic board (100 mm × 100 mm × 20 mm, WHD) based on the CAD file. In this study, sharp edge short end mills (MSES230P, NS TOOL) whose diameters is 200 μm is utilized to slot the microchannel whose width and depth are 200 and 170 μm, respectively. The inlet and two outlet ports are throughholes which are connected to a microfeeder (IC3210, KD Scientific) and sample bottles through tubes from the other side of the board. The channels are covered with another acrylic board (100 mm × 100 mm × 10 mm, WHD) and these two boards are affixed tightly by using nuts and bolts.

In this study, suspensions whose weight concentration is 0.06 wt.% are prepared using ion-exchanged water and acrylic particles (MR-7G, MR-10GH, MR-20G, Soken Chemical & Engineering) whose density is 1190 kg/m^3 and average diameters are 7, 10 and 20 μm, respectively. The speed of microfeeder is adjusted to obtain a desired Reynolds number *Re* in the range 150–600 based on the equivalent diameter of the channel. Weight, absorbance at 900 nm (PD-303, APEL) and particle size distribution (SALD-200V ER Model 2, SHIMADZU) of samples collected from inner and outer exits are measured in the present study to examine the feasibility.

4.2. Results and discussion

Fig. 12 shows the volume-based particle size distributions of samples collected from the inner and the outer exits at $De = 40$ ($Re = 600$) for the 10 μm particles. Although the lower limits of both samples are the same due to the Dean vortices, the upper limit of inner sample is clearly smaller than that of outer sample. It can be seen further that the peak positions are significantly different, viz. 7.5 and 13.4 μm for inner and outer samples, respectively. It was observed that PSD of each outer sample existed in nearly the same or a slightly smaller range compared with that of the feed sample. This seems to be because larger particles settled as was observed in a tube between the device and microfeeder or in a syringe where the fluid velocity was too slow to lift

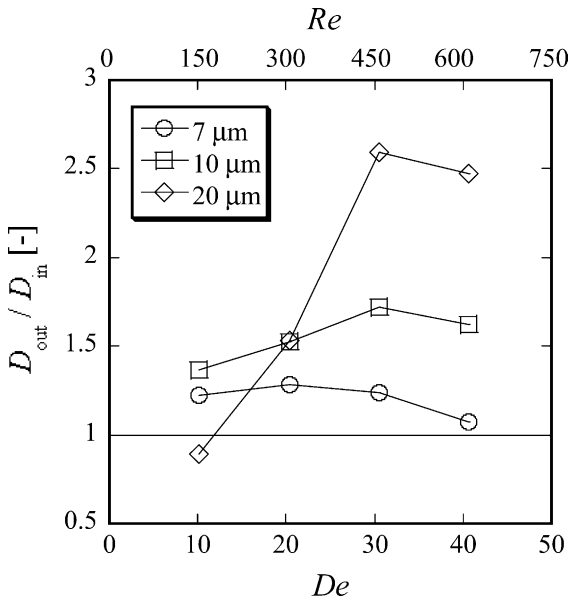

Fig. 13. The dependency of classification effect index D_{out}/D_{in} on *De*.

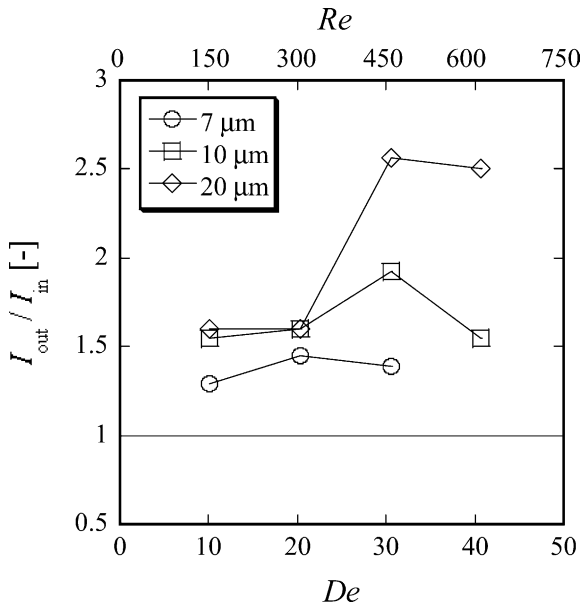

Fig. 14. The dependency of concentration effect index I_{out}/I_{in} on *De*.

and carry the particles into the device. Therefore, it is not possible to determine the PSD of feed sample that actually enters the device. The problem should be solved for the exact evaluation of the device performance by means of a new approach in future.

The ratio of average diameters of those samples D_{out}/D_{in} is utilized as an index of classification in this study. Fig. 13 shows the dependency on *De* of the ratios of average diameter of samples collected from inner and outer exits D_{out}/D_{in} for all the particles. It can be seen that the indices increase in the range of *De* below 30 but slightly decrease at $De = 40$ for the 10 and 20 μm particles. The index for the 7 μm particles begins to decrease at $De = 20$. It is also clear that the classification efficiency increases with the particle size. The dependency on the particle size is possibly brought about by the difference of the relative velocity between larger particles and suspending medium as discussed above.

Fig. 14 shows the dependency on *De* of the ratios of absorbance of samples collected from inner and outer exits I_{out}/I_{in} for the all particles. Since the absorbance is proportional to the particle number density and the absorbance coefficient depends on the size, it was not possible to determine the weight concentration of each sample based on the measured absorbance due to the varied PSD and unknown absorbance coefficients. It is generally expected that the weight concentration ratio is possibly higher than the absorbance ratio, I_{out}/I_{in}, since the absorbance of a sample containing larger particles would be lower than that of a sample containing smaller particles even if their weight concentrations are same. The dependency of I_{out}/I_{in} on *De* is almost the same as that of D_{out}/D_{in}. It is also supposed that the dependency of the index on the particle size is brought by the relative velocity difference between different sized particles.

Based on those experimental results, it can be concluded that the curved microchannel with a bifurcation at one end works for the classification of contained particles and concentration of the slurry in the examined *De* range. It should be noted that more severe indices of classification and concentration effects, viz. D_{out}/D_{in} and I_{out}/I_{in}, were adopted instead of mode diameter and weight concentration ratios, respectively, although the separation efficiency curve could not be determined because of aforementioned reasons.

5. Conclusions

It is confirmed numerically that the Dean vortices appear in the microchannel whose width, depth and curvature radius are 200 μm, 170 μm and 20 mm, respectively, in the examined flow rate range, viz. $Re = 150$, 300, 450 and 600 ($De = 10$, 20, 30 and 40) for water. Correlations of acceleration with mean tangential velocity and of the Dean vortices velocity with *De* number are proposed for the examined microchannel. It is also verified numerically that acceleration is sufficiently high to bring concentration effect and Dean vortices are established rapidly after entering the curved section and several circulations can be expected to exhibit the re-dispersion effect. In addition to the numerical confirmation of the feasibility, experimental evidence of classification and concentration effects in the corresponding condition examined in the numerical simulation is shown. It is finally concluded that the feasibility of a newly developed micro-separator/classifier is well verified numerically and experimentally. The coupled particle and fluid flow modeling is required for the optimization of the performance. This will be the topic of study for further work. The benchmarking of the performance that will be achieved after the

optimization should be carried out based on the separation efficiency curve that would be obtained by a new approach.

Acknowledgements

The authors are most grateful to Prof. Chiaki Kuroda at Tokyo Institute of Technology for his valuable advice on the present study.

References

[1] S. Sugihara, M. Nakajima, M. Seki, Preparation of monodispersed polymeric microspheres over 50 μm employing microchannel emulsification, Ind. Eng. Chem. Res. 41 (2002) 4043–4047.
[2] H. Wang, H. Nakamura, M. Uehara, M. Miyazaki, H. Maeda, Preparation of titania particles utilizing the insoluble phase interface in a microchannel reactor, Chem. Commun. (2002) 1462–1463.
[3] T. Kawakatsu, Y. Kikuchi, M. Nakajima, Regular-sized cell creation in microchannel emulsification by visual microprocessing method, J. Am. Oil Chem. Soc. 74 (1997) 317–321.
[4] J.J. Cilliers, S.T.L. Harrison, The application of mini-hydrocyclones in the concentration of yeast suspensions, Chem. Eng. J. 65 (1997) 21–26.
[5] J.P. Shelby, D.S.W. Lim, J.S. Kuo, D.T. Chiu, High radial acceleration in microvortices, Nature 425 (4) (2003) 38.
[6] A. Einstein, Eine neue Bestimmung der Moleküldimensionen, Ann. Phys. 19 (1906) 289–306.
[7] A. Einstein, Berichtigung zu meiner arbeit: Eine neue Bestimmung der Moleküldimensionen, Ann. Phys. 34 (1911) 591–592.
[8] S. Ookawara, R. Higashi, D. Street, K. Ogawa, The Influence of Channel Depth on the Performance of a Micro-Separator/Classifier. Kagaku Kogaku Ronbunshu, submitted for publication.
[9] W.R. Dean, Fluid motion in a curved channel, Proc. R. Soc. London Ser. A 121 (1928) 402–420.
[10] K.Y. Chung, G. Belfort, W.A. Edelstein, X. Li, Dean vortices in curved tube flow. 5. 3-D MRI and numerical analysis of the velocity field, AIChE J. 39 (1993) 1060–1592.